Microscopic Observation of Kinetic Molecular Sieving of Hydrogen Isotopes in a Nanoporous Material

T. X. Nguyen,[1] H. Jobic,[2] and S. K. Bhatia[1,*]

[1]School of Chemical Engineering, The University of Queensland, Brisbane, Queensland 4072, Australia
[2]Université Lyon 1, CNRS, UMR 5256, IRCELYON, Institut de recherches sur la catalyse et l'environnement de Lyon, 2 Avenue Albert Einstein, F-69626 Villeurbanne, France

(Received 11 May 2010; revised manuscript received 24 June 2010; published 19 August 2010)

We report quasielastic neutron scattering studies of H_2-D_2 diffusion in a carbon molecular sieve, demonstrating remarkable quantum effects, with the heavier isotope diffusing faster below 100 K, confirming our recent predictions. Our transition state theory and molecular dynamics calculations show that while it is critical for this effect to have narrow windows of size comparable to the de Broglie wavelength, high flux requires that the energy barrier be reduced through small cages. Such materials will enable novel processes for kinetic molecular sieving of hydrogen isotopes.

DOI: 10.1103/PhysRevLett.105.085901 PACS numbers: 66.30.Pa, 28.60.+s, 68.43.Jk, 83.10.Rs

The molecular sieving of isotopes has been considered impossible because of their similar size and shape, and energy intensive cryogenic distillation or thermal diffusion have been considered more promising for H_2 isotope separation [1]. While the possibility of harnessing quantum effects in molecularly sized nanopores to achieve the equilibrium separation of light isotopes such as hydrogen and deuterium has been theoretically recognized [2–5], its experimental confirmation is awaited. Quantum separation is facilitated by the larger de Broglie wavelength of the lighter isotope, which becomes comparable to the space available for molecular motion at sufficiently low temperatures, and restricts its adsorption. Perhaps even more remarkable is the prediction that the quantum effect leads to the heavier isotope, D_2, diffusing faster than H_2 in nanoporous zeolite rho [6,7], with crossover in diffusivities at 94 K. Faster particle scale uptake of D_2 compared to H_2 at 77 K has since been observed in gravimetric adsorption studies [8,9] with carbon molecular sieves and a metal organic framework material, albeit with unknown controlling mechanism, but no microscopic evidence for such quantum effects on the transport has been found.

Here, we report the first microscopic observations of faster diffusion of D_2 compared to H_2 in a nanoporous carbon molecular sieve, obtained using quasielastic neutron scattering. Our interpretations of the data using transition state theory and molecular dynamics simulations demonstrate that increasingly larger pores contribute to this effect as the temperature is reduced. We find that while it is critical to this effect to have sufficiently narrow pore windows, high flux requires that the cages interconnected by these windows must also be small. These results open the door for optimal design and synthesis of adsorbents for new isotope separation processes using kinetic molecular sieving mediated by quantum effects.

The quasielastic neutron scattering (QENS) measurements were performed on the time-of-flight spectrometer IN6, at the Institut Laue-Langevin. The incident neutron energy was taken as 3.12 meV, corresponding to a wavelength of 5.1 Å. The elastic energy resolution is given by a Gaussian function, with a half width at half maximum (HWHM) of the order of 40 μeV. The diffusion of molecules can be characterized from the broadening of the elastic peak (see Fig. 1), the larger the broadening the larger the diffusivity [10–12]. Our analysis of the QENS spectra fits a Lorentzian function in energy, of HWHM, $\Delta\omega$, to the experimental dynamical structure factor, $S(Q, \omega)$, obtained at small values of the wave-vector transfer, Q [10–12]. In particular, the analysis of the spectra was performed at $Q = 0.486$ Å^{-1} in Fig. 1, probing sufficiently large distances compared to the length of elementary jumps, so that the diffusion process can be described by Fick's second law [10]. Under these conditions, $\Delta\omega$ is simply DQ^2, so that the diffusion coefficient D can be obtained [12] from the broadening as a function of Q^2. Furthermore, our QENS measurements were carried out at very low loading (0.5 mmol/g), at which self- and transport diffusivities are essentially identical [12]. Figure 1 showed excellent fits of Lorentzian functions (solid lines), after convolution with the instrumental resolution, to the experimental dynamical structure factors of H_2 (red crosses) and D_2 (blue crosses) in Takeda 3 Å carbon molecular sieve (CMS) for four temperatures: 30, 50, 77, and 120 K. Only the wings of the QENS spectra were fitted [13] because the subtraction of the signal of the degassed CMS, which showed large small-angle scattering, influences the elastic intensity. It is also evident that the shapes of the fitted Lorentzian functions obtained for D_2 are broader than those for H_2 at all the temperatures below 120 K, indicating faster diffusion of D_2 compared to H_2 in the CMS. This difference in width increases with the decrease in temperature, indicative of a larger decrease in the diffusivity of H_2 compared to D_2. Further details of the QENS experiment and data analysis are provided in the supplementary material [13].

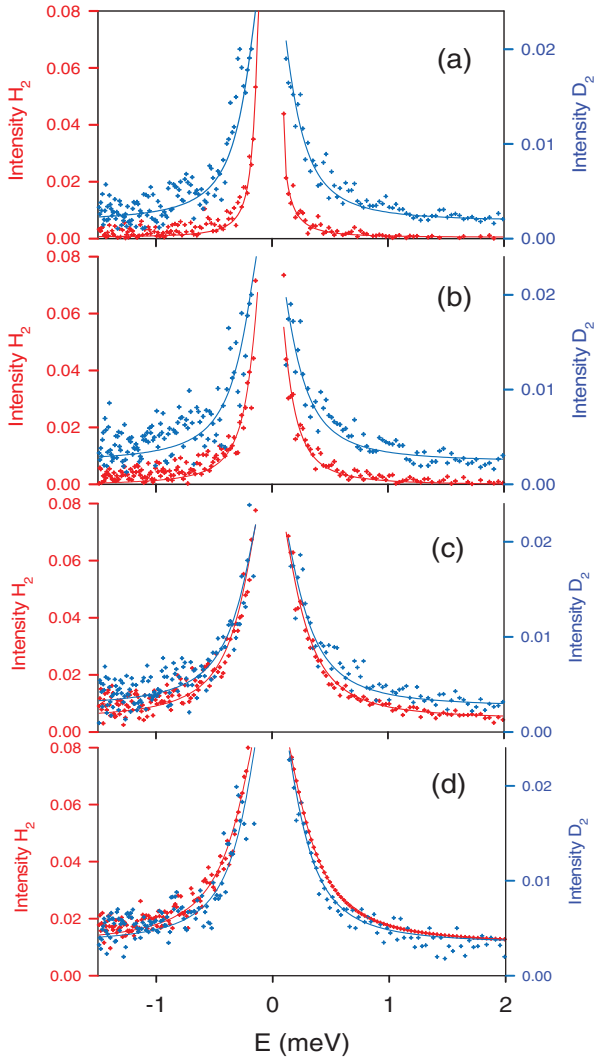

FIG. 1 (color). Comparison between experimental and calculated QENS spectra obtained for H_2 and D_2 in Takeda 3 Å CMS, at different temperatures: (a) 30 K, (b) 50 K, (c) 77 K, (d) 120 K (loading: 0.5 mmol/g, $Q = 0.486$ Å^{-1}). These spectra correspond to the grouping of 10 detectors ranging from 0.454 to 0.525 Å^{-1}.

Figure 2 depicts the temperature variation of the self-diffusivity of H_2 and D_2 in the CMS over the temperature range 30–140 K. Taking into account values from refinements using different groupings of detectors, typical mean errors of 15% and 25% were estimated for H_2 and D_2, respectively. A crossover of the diffusivities at 100 K is evident, with D_2 diffusing faster than H_2 below this temperature. Above 100 K it is the H_2 that diffuses faster, as can be seen from a comparison between Figs. 1(c) and 1(d). We have theoretically shown [7], using a Feynman-Hibbs (FH) path integral formalism [14], that the quantum leads to faster diffusion of D_2 compared to H_2 below 94 K, in zeolite rho having a narrow window diameter of 0.543 nm. The pore window diameter or size is defined as the surface atom center-center distance, and after subtracting the collision diameter of a solid atom, this provides an open diameter of 0.27 nm (considering [15] a surface oxygen diameter of 0.27 nm). This matches well with the primary peak in the pore size distribution (PSD) of the CMS [16], depicted in inset (a) of Fig. 2. Consequently, the excellent correspondence of the experimental and theoretical crossover temperatures is a strong confirmation of the importance of the quantum effect, and its role in the faster reduction of the diffusivity of H_2 with decrease in temperature. A faster decrease of the diffusivity of H_2 is also predicted for high temperature amorphous metal membranes [17].

As reference data, inset (b) of Fig. 2 depicts experimental QENS-based diffusivity data and molecular dynamics simulation results for H_2 self-diffusion in zeolite rho at various temperatures in the range 30–140 K [7]. The excellent agreement when quantum effects are considered confirms the accuracy of the QENS experiments and their sensitivity to the quantum effect.

To examine the conditions that lead to the faster diffusion of D_2 we employ transition state theory (TST) to the trajectories of molecules crossing the energy barrier at narrow windows connecting molecular scale pore bodies or cages. TST provides the ratio of diffusivities [18].

$$\frac{D_s(\mathrm{D_2})}{D_s(\mathrm{H_2})} = \left(\frac{m_{\mathrm{H_2}}}{m_{\mathrm{D_2}}}\right)^{1/2} e^{(E_a^{\mathrm{H_2}} - E_a^{\mathrm{D_2}})/k_B T} = \frac{1}{\sqrt{2}} e^{(E_a^{\mathrm{H_2}} - E_a^{\mathrm{D_2}})/k_B T}. \quad (1)$$

At sufficiently low temperature and density the activation barrier is governed by the difference in solid-fluid interaction energy between the saddle point (U^*) and the binding site in the cage (U^b) [19,20], i.e., $E_a = U^* - U^b$. For sufficiently high temperatures (>40 K), we may model the quantum effect using the second order expansion of the FH path integral [14]. Use of a Lennard-Jones (LJ)

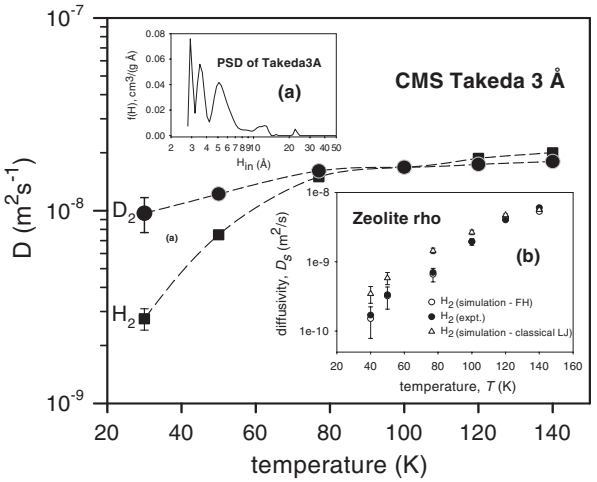

FIG. 2. Diffusion coefficients for H_2 and D_2 in Takeda 3 Å CMS, as a function of temperature (loading: 0.5 mmol/g), showing typical error bars. Inset (a) depicts the pore size distribution of the CMS obtained [13] from the interpretation of experimental high pressure CO_2 adsorption data. Inset (b) depicts experimental and molecular dynamics simulation results for self-diffusivity of H_2 in zeolite rho [7].

potential for the C-H_2 or C-D_2 interaction yields [18]

$$\ln\left(\sqrt{2}\frac{D_s(\mathrm{D_2})}{D_s(\mathrm{H_2})}\right) = \frac{E_a^{\mathrm{H_2}} - E_a^{\mathrm{D_2}}}{k_B T} = \frac{A}{T^2}, \tag{2}$$

where $A = \hbar^2 F_2(r_{*b})/k_B(\Delta\mu)\sigma_{sf}^2$, representing a quantum separation factor dependent only on the intrinsic properties of the adsorption system. Here $\Delta\mu = \mu_{\text{C-H}_2}\mu_{\text{C-D}_2}/(\mu_{\text{C-D}_2} - \mu_{\text{C-H}_2})$, and $\mu_{X\text{-}Y} = m_X m_Y/(m_X + m_Y)$. σ_{sf} is the LJ length scale parameter. $F_2(r_{*b})$ is a function that depends on the difference in the strength of the interaction between the pore mouth and the cage, and is given by

$$F_2(r_{*b}) = \sigma_{sf}^2[n_* f_2(r_*) - n_b f_2(r_b)] \quad \therefore$$
$$f_2(r_x) = \frac{5\varepsilon_{sf}}{\sigma_{sf}^2}\left[4.4\left(\frac{\sigma_{sf}}{r_x}\right)^{14} - \left(\frac{\sigma_{sf}}{r_x}\right)^{8}\right], \tag{3}$$

where n_* is the number of carbon atoms surrounding the saddle point located at a distance r_*, and n_b the number of carbon atoms closest to the binding site in the cage and located at a distance r_b. Equation (2) is a remarkable result, showing inverse quadratic temperature dependence due to quantum effects, as opposed to the Arrhenius temperature dependence expected from a classical activated barrier crossing process. Figure 3 shows the excellent linear fit of Eq. (2) to the experimental self-diffusivity data for H_2 and D_2 (Fig. 2), validating the quantum effect; with the slope yielding the quantum separation factor A.

The inset of Fig. 3 depicts the function $\sigma_{sf}^2 f_2(r)$ for the CMS, based on which the function $F_2(r_{*b})$ can be estimated [18]. From the inset, it is readily seen that the quantum separation factor, A, is governed by the window size (0.566 nm). Crossover occurs for sufficiently small windows if the cage size is such that $r_b > \sigma_{sf}$. To investigate whether the cage size has a significant effect on the

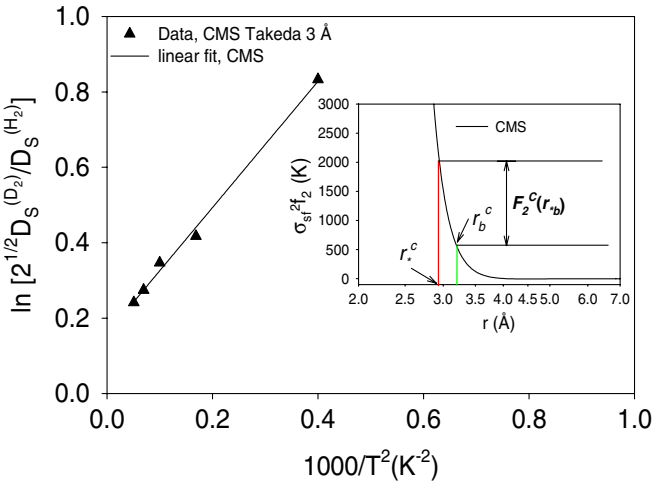

FIG. 3 (color online). Linear fit of Eq. (2) to experimental data of self-diffusivity of hydrogen isotopes in CMS Takeda 3 Å. The inset depicts the value of $F_2(r_{*b})$ for CMS Takeda 3 Å (F_2^{C}). Here r_x^y is the radius of cage ($x = b$) and window or pore mouth ($x = *$) in CMS Takeda 3 Å ($y = \mathrm{C}$).

self-diffusivity of H_2 isotopes, we calculated their activation energy ($E_a = U^* - U^b$) at 50 K in carbon models having various cage sizes but similar window size of 0.566 nm. The large cages were represented by fullerenes, C_{60}, C_{78}, and C_{90}, that have center-center diameters of 0.71, 0.81, and 0.87 nm, respectively. The radius r_b of these large cages is such that $r_b \geq 2^{1/6}\sigma_{sf}$. We also examined the case of a small cage created by removing carbon atoms from the opposing walls of a slit pore, as illustrated in Fig. 4(a), which has only 6 carbon atoms and a diameter of 0.632 nm. Calculations showed that the activation energy E_a for the carbon models with the large cages lies in the range of 5756–6075 K, and is 1.5–1.6 times larger than that of the carbon model with the small cage size. This leads to significant retardation of the diffusion of H_2 isotopes in the large cage carbon models compared to that in the smaller cage model. Thus, we conclude that the optimal microstructure of porous materials for kinetic separation of H_2 isotopes based on the quantum effect must contain small windows and cages whose radii, r_* and r_b respectively, are such that r_* is sufficiently smaller than σ_{sf}, while r_b is slightly larger σ_{sf} and in the neighborhood of the distance at which the solid-fluid interaction approaches zero. This condition leads to a significantly large quantum separation factor A, without high activation energy barrier.

Equilibrium molecular dynamics (EMD) simulations were next conducted to determine the self-diffusivities of H_2 and D_2 in a synthetic model carbon with defective slitlike pores. This model carbon comprises two parallel graphitic sheets separated by a carbon-carbon distance corresponding to pore size H_{CC}. The size of the slit pore ($H_{CC} < 0.588$ nm), is sufficiently small to be slightly repulsive to a hydrogen isotope molecule. Accordingly, if carbon atoms are symmetrically removed from the two opposing carbon walls in an identical manner, as illustrated in Fig. 4(b), cages which can accommodate a hydrogen isotope molecule are formed between carbon atoms that are nearest neighbors of the missing atoms. The open space between the remaining atoms on the opposing walls now provides the window for entry into the cages, and in this way cage-window pairs are created. The pore volume of the carbon model approximates that of the actual Takeda 3 Å CMS of 0.17 $\mathrm{cm^3/g}$. Figure 4 depicts the carbon model which consists of binding sites (centers of cages) separated by dividing surfaces (broken lines). Hydrogen isotope molecules (H_2 and D_2) and carbon atoms are modeled as effective LJ spheres. The Lennard-Jones (12-6) potential is employed to model sorbate-sorbate and sorbate-carbon interactions, with the fourth order expansion of the semiclassical Feynman-Hibbs potential [5,6] representing quantum effects. For the H_2-H_2 and D_2-D_2 interactions we used the LJ parameters $\sigma_f = 0.2958$ nm and $\varepsilon_f/k_B = 36.7$ K, and for the C-C interaction we used the flat surface parameters [16] $\sigma_c = 0.34$ nm and $\varepsilon_c/k_B = 37.26$ K. LJ sorbate-carbon parameters were determined based on the Berthelot mixing rules. The EMD

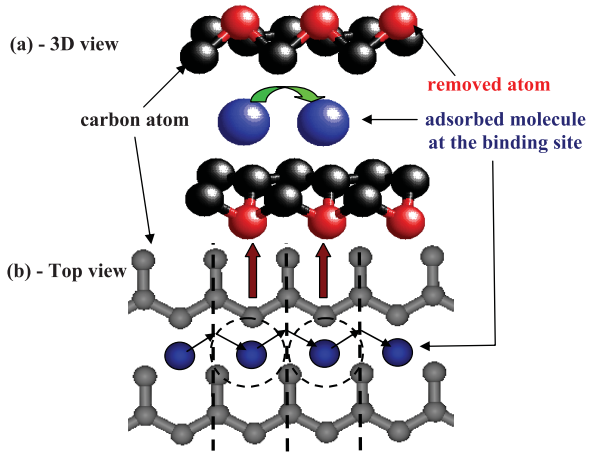

FIG. 4 (color). (a) 3D view of periodic slitlike carbon model containing 240 carbon atoms. Diffusion path (bending arrows) shows movement of fluid molecules. (b) A top view of one pore wall of the carbon model with carbon atoms removed [red spheres in (a)] to create cages, showing the diffusion path of an adsorbed molecule through neighboring cages (broken circle), and through the dividing surface (vertical dashed line).

simulations used a 0.3 fs time step, with total run length typically 120 ns. Each run consists of 3 molecules in a unit cell which approximates the experimental loading of 0.5 mmol/g. The self-diffusivity is determined from the particle velocity autocorrelation function (VACF). Crossover of the diffusivities of H_2 and D_2 was observed in the model carbon in the low temperature range of 30–100 K, at temperature-dependent ultramicropore sizes, H_{CC}, less than 5.9 Å. Our results [18] showed that the experimental diffusivities of H_2 and D_2 could be reasonably matched by the simulations, but with a pore width that decreased with increasing temperature. Thus, at 30 K the effective pore width was 0.588 nm, while at 50 K it was 0.566 nm and at 77 K it was 0.54 nm. From these results we conclude that at the lowest temperature (30 K) the diffusion is governed by transport through pores having wider pore mouths, because of the relatively low associated energy barrier; however, with an increase in temperature the higher kinetic energy leads to increase in contribution of narrower pore mouths offering higher energy barriers. The effective pore widths, in the range of 5.4–5.88 Å (C-C distances) for temperatures of 30–77 K, clearly fall within the first peak of the pore size distribution (based on open pore width) depicted in the inset of Fig. 2, considering a carbon atom diameter of 3.4 Å. This confirms that the first peak of the PSD represents the pore entrances or windows between neighboring pore bodies (i.e., cages) in the CMS structure.

In conclusion, quantum kinetic sieving of hydrogen isotopes (H_2 and D_2) has been microscopically observed in Takeda 3 Å CMS at low temperatures (<100 K), with D_2 diffusing faster than H_2 below 100 K. Our transition state theory and equilibrium molecular dynamics based interpretations of the data indicate that carbonaceous molecular sieves hold promise as adsorbent materials or membranes for the separation of H_2 isotopes by quantum kinetic sieving. The key to an optimal material is to have both a small pore mouth, to provide a strong quantum effect, and small cage size, so as to achieve high flux by minimizing the energy barrier. The design and synthesis of improved materials with these properties will lead to new adsorptive separation process for light isotopes. The production of heavy water by adsorptive D_2O-H_2O separation is another tantalizing prospect for application of the above concepts.

We acknowledge funding of this research by the Australian Research Council. We thank Dr. M. M. Koza for his help during the measurements on the IN6 spectrometer at the Institut Laue-Langevin, Grenoble, France.

*To whom correspondence should be addressed.
s.bhatia@uq.edu.au

[1] G. Văsaru, *Tritium Isotope Separation* (CRC Press, Boca Raton, 1993).
[2] J. J. M. Beenakker, V. D. Borman, and S. Y. Krylov, Chem. Phys. Lett. **232**, 379 (1995).
[3] Q. Y. Wang, S. R. Challa, D. S. Sholl, J. K. Johnson, Phys. Rev. Lett. **82**, 956 (1999).
[4] H. Tanaka, D. Noguchi, A. Yuzawa, T. Kodaira, H. Kanoh, and K. Kaneko, J. Low Temp. Phys. **157**, 352 (2009).
[5] Y. Wang and S. K. Bhatia, J. Phys. Chem. C **113**, 14953 (2009).
[6] A. V. Anil Kumar and S. K. Bhatia, Phys. Rev. Lett. **95**, 245901(2005); **96**, 119901(E) (2006).
[7] A. V. A. Kumar, H. Jobic, and S. K. Bhatia, J. Phys. Chem. B **110**, 16 666 (2006).
[8] X. B. Zhao, S. Villar_Rodil, A. J. Fletcher, and K. M. Thomas, J. Phys. Chem. B **110**, 9947 (2006).
[9] B. Chen, X. B. Zhao, A. Putkham, K. Hong, E. B. Lobkovsky, E. J. Hurtado, A. J. Fletcher, and K. M. Thomas, J. Am. Chem. Soc. **130**, 6411 (2008).
[10] M. Bée, *Quasielastic Neutron Scattering* (Hilger, Bristol, 1998).
[11] H. Jobic, J. Kärger, and M. Bée, Phys. Rev. Lett. **82**, 4260 (1999).
[12] H. Jobic and D. N. Theodorou, Microporous Mesoporous Mater. **102**, 21 (2007).
[13] See supplementary material at http://link.aps.org/supplemental/10.1103/PhysRevLett.105.085901 for experimental details and discussion of data analysis.
[14] R. P. Feynman and A. R. Hibbs, *Quantum Mechanics and Path Integrals* (McGraw-Hill, New York, 1965).
[15] D. W. Breck, *Zeolite Molecular Sieves* (John Wiley and Sons, New York, 1974).
[16] T. X. Nguyen, J. S. Bae, Y. Wang, and S. K. Bhatia, Langmuir **25**, 4314 (2009).
[17] L. Semidey-Flecha, S. Hao, and D. S. J. Sholl, J. Taiwan Inst. Chem. Eng. **40**, 246 (2009).
[18] See supplementary material at http://link.aps.org/supplemental/10.1103/PhysRevLett.105.085901 for details.
[19] A. F. Voter and J. D. Doll, J. Chem. Phys. **80**, 5832 (1984).
[20] T. X. Nguyen and S. K. Bhatia, J. Phys. Chem. C **111**, 2212 (2007).